Available online at www.sciencedirect.com
SCIENCE DIRECT®
Physics Letters A 346 (2005) 217–221
PHYSICS LETTERS A
www.elsevier.com/locate/pla

Magnetic and transport properties of $La_{0.7}Te_{0.3}CrO_3$

J. Yang [a,b,*], Y.Q. Ma [a], B.C. Zhao [a], R.L. Zhang [a], W.H. Song [a], Y.P. Sun [a]

[a] *Key Laboratory of Materials Physics, Institute of Solid State Physics, Chinese Academy of Sciences, Hefei 230031, People's Republic of China*
[b] *School of Materials Science and Engineering, Wuhan University of Technology, 122 Luoshi Road, Wuhan 430070, People's Republic of China*

Received 4 January 2005; received in revised form 24 July 2005; accepted 26 July 2005

Available online 3 August 2005

Communicated by R. Wu

Abstract

The structural, magnetic and transport properties in the compound $La_{0.7}Te_{0.3}CrO_3$ have been investigated. The sample shows an orthorhombic structure with the space group *Pbnm*. The sample exhibits two magnetic transitions corresponding to the transition from a paramagnetic (PM)–antiferromagnetic (AFM) transition at 282 K, and an AFM–ferromagnetic (FM) transition at about 105 K, which is presumed to originate from the exchange interaction between Cr^{2+} and Cr^{3+} ions mediated by O^{2-} ions. The temperature dependence of resistivity $\rho(T)$ curve displays the semiconducting behavior ($d\rho/dT < 0$) over whole measured temperature range. Based on the results of the magnetic and transport properties in $La_{0.7}Te_{0.3}CrO_3$, it is suggested that the exchange interaction of Cr^{2+}–O–Cr^{3+} is of the nature of superexchange interaction rather than double exchange interaction.

PACS: 75.30.Et; 75.30.Kz; 75.50.Gg

Keywords: Magnetically ordered materials; Phase transition; Electric transport

Lanthanum chromate $LaCrO_3$ is a perovskite-type compound. It has an orthorhombic structure with the space group *Pnma* at the room temperature. The single-phase $LaCrO_3$ has a *G*-type antiferromagnetic (AFM) structure with inter- and intralayer antiparallel spin alignments and Néel temperature (T_N) of 280 K [1–3]. The compounds $La_{1-x}A_xCrO_3$ (A is a divalent element such as Ca, Sr, etc.) have recently received much interest as electrode materials or interconnection for solid oxide electrolyte fuel cells (SOFC) because of their high electronic conductivity in the fuel and oxidant atmospheres [4,5]. Although much research on the thermodynamics, conductivity, and sinterability of these compounds has been reported [6–11], to our best knowledge, there are few reports as to the magnetic properties of these compounds, especially for the com-

* Corresponding author. Tel.: +86 551 5591439; fax: +86 551 5591434.
E-mail address: jyang@issp.ac.cn (J. Yang).

0375-9601/$ – see front matter
doi:10.1016/j.physleta.2005.07.066

pound $La_{0.7}Te_{0.3}CrO_3$ where Te^{4+} ions are used to substitute La^{3+} ions. For $La_{0.7}Te_{0.3}CrO_3$, the mixed-valence state of Cr^{2+}–Cr^{3+} is introduced for the sake of the charge neutrality. We noticed that Cr^{2+}/Cr^{3+} ions has the identical electronic configuration with Mn^{3+}/Mn^{4+} ions, which has been suggested to be a key component for understanding the colossal magnetoresistance (CMR) effect and the transition from the paramagnetic (PM) insulator–ferromagnetic (FM) metal for the hole-doped magnanites $Ln_{1-x}A_xMnO_3$ (Ln = La–Tb, and A = Ca, Sr, Ba, Pb, etc.). Thus, an interesting question is easily mentioned: can the mixed-valence state of Cr^{2+}/Cr^{3+} induce the PM–FM transition and the CMR effect in $La_{0.7}Te_{0.3}CrO_3$? With this notion in mind, in the Letter, we report our investigations as to the structural, magnetic and transport properties of $La_{0.7}Te_{0.3}CrO_3$.

It is well known that it is difficult to sinter $LaCrO_3$ to high density at high oxygen pressure [11]. In this work, the sol-gel method similar to the one presented by Verelst et al. [12] has been used to synthesize $La_{0.7}Te_{0.3}CrO_3$, since this procedure can enhance the density and phase homogeneity of the sample at lower temperatures. Stoichiometric amounts of high-purity La_2O_3 and TeO_2 powders were dissolved in diluted nitric acid in which an excess of citric acid was added, followed by the addition of stoichiometric amounts of Cr $(NO_3)\cdot 9H_2O$ dissolved in distilled water with continuous stirring, and then ethylene glycol was added to make a solution complex. After all reactants had been completely dissolved, the solution was heated on a hot plate resulting in the formation of a gel. The gel was dried at 250 °C, and then preheated to 600 °C to remove the remaining organic and decompose the nitrates of the gel. The obtained powders were ground, palletized, and sintered at 1100 °C for 24 h, and finally, the furnace was slowly cooled down to the room temperature. The chemical composition of the sample was determined by energy dispersive spectroscopy (EDS) quantitative analysis with scanning electron microscope (AMRAY 1000B). The nominal $La_{0.7}Te_{0.3}CrO_3$ could be viewed as $La_{0.71}Te_{0.29}Cr_{0.98}O_3$ with error limits less than 3%. The oxygen content of the sample was determined by a redox (oxidation reduction) titration. The detailed method to determine the oxygen content of sample is reported in elsewhere [13], and the oxygen content of the sample can be determined as 3.01.

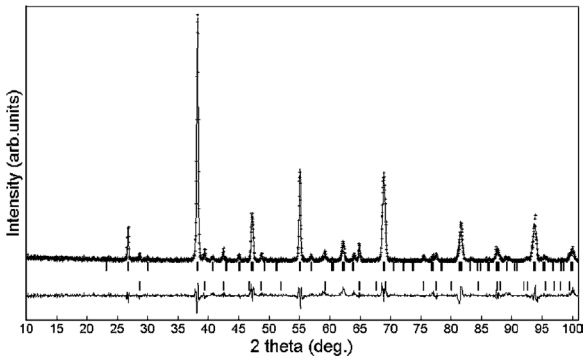

Fig. 1. XRD patterns of the compound $La_{0.7}Te_{0.3}CrO_3$. Crosses indicate the experimental data and the calculated data is the continuous line overlapping them. The lowest curve shows the difference between experimental and calculated patterns. The upper and lower vertical bars indicate the expected reflection positions for the orthorhombic phase $La_{0.7}Te_{0.3}CrO_3$ and the rhombohedral phase Cr_2O_3, respectively.

The crystal structures were examined by X-ray diffractometer using Co radiation at the room temperature. The magnetization measurements were carried out with a quantum design superconducting quantum interference device (SQUID) MPMS system ($2 \leqslant T \leqslant 400$ K, $0 \leqslant H \leqslant 5$ T). Both zero-field-cooled (ZFC) and field-cooled (FC) data were recorded. The resistance was measured by the standard four-probe method.

Fig. 1 shows XRD pattern of $La_{0.7}Te_{0.3}CrO_3$ sample. It is found that the sample has an orthorhombic lattice with the space group *Pbnm*, and traces of Cr_2O_3 (< 5%) have been taken into account. The structural parameters can be obtained by fitting the experimental spectra using the standard Rietveld technique [14] and the results are listed in Table 1. The compound $La_{0.7}Te_{0.3}CrO_3$ is a two-phase composed of the orthorhombic phase ($La_{0.7}Te_{0.3}CrO_3$) and the rhombohedral phase (Cr_2O_3) with the lattice parameters $a = 4.9597$ Å, and $c = 13.5902$ Å.

Fig. 2(a) and (b) show the temperature dependence of magnetization M of $La_{0.7}Te_{0.3}CrO_3$ under both ZFC (M_{ZFC}) and FC (M_{FC}) modes at $H = 0.1$ T and 1 T, respectively. Our measured sample may be considered as ellipsoid in which the demagnetization factor $N = 0.05$ (SI units), and the applied field is parallel to the longest semi-axis of sample. So a uniform field can exist throughout the sample and the shape demagnetization field can be reduced as much as possible.

Table 1
Refined structural parameters of $La_{0.7}Te_{0.3}CrO_3$ at room temperature. O(1): apical oxygen; O(2): basal plane oxygen

Atom	Position	x	y	z
La, Te	4(c)	0.4952	0.0192	0.25
Cr	4(a)	0	0	0
O(1)	4(c)	0.5980	0.4984	0.25
O(2)	8(d)	0.2462	0.2938	0.0562
$a = 5.5002$ Å				
$b = 5.4810$ Å				
$c = 7.7657$ Å				
$V = 234.1121$ Å^3				
$R_P = 9.81$				
$R_{wp} = 12.62$				
$\chi^2 = 1.77$				
Cr–O(1) = 2.0149 Å	Cr–O(2) = 1.7748 Å	Cr–O(2) = 2.2132 Å	(Cr–O) = 2.0010 Å	
Cr–O(1)–Cr = 148.96°	Cr–O(2)–Cr = 153.50°	(Cr–O–Cr) = 151.99°		

From Fig. 2(a) and (b), we can see that $La_{0.7}Te_{0.3}CrO_3$ sample exhibits two magnetic transitions under applied fields of 0.1 T and 1 T. Additionally, there exist distinct differences between M_{FC} and M_{ZFC} curves below the higher magnetic transition temperature for both cases. The M_{ZFC} curve exhibits a broad peak around 100 K in a field of 0.1 T, whereas in the case of 1 T, the M_{ZFC} curve shows a broad peak around 80 K and the differences between the M_{FC} curve and the M_{ZFC} one become smaller compared with that in a field of 0.1 T. This large discrepancy between the M_{FC} and M_{ZFC} curve, and the field dependence of the M_{ZFC} curve at low temperatures are reminiscent of a characteristic of cluster glass [15]. Fig. 2(c) shows the temperature dependence of the inverse magnetic susceptibility χ_m for the sample $La_{0.7}Te_{0.3}CrO_3$. It can be seen that in the temperature region of 290–315 K, the relation between χ_m and the temperature T follows the Curie–Weiss law, i.e., $\chi_m = C/(T - \Theta)$, where C is the Curie constant, and Θ is the Weiss temperature. The effective magnetic moment of $1.67\mu_B$ can be deduced from the Curie–Weiss fitting. This value is obviously lower than expected value of $4.18\mu_B$ based on spin-only contributions of Cr^{3+} ($S = 3/2$) and Cr^{2+} ($S = 2$). It implies that there may exist a strong spin–orbit coupling in $La_{0.7}Te_{0.3}CrO_3$ leading to the gyromagnetic factor less than 2. The Weiss temperature Θ is thus estimated to be around -190 K according to the extrapolation lines of the fitting curves as shown in Fig. 2(c). So we concluded that this magnetic transition corresponds to PM to AFM transition. Additionally, It can be seen that the value of $1/\chi_m$ begin to drop abruptly from the temperature of 315 K and keep almost constant above 315 K, which may be related to the existence of the minor impurity Cr_2O_3. The magnetic transition temperature is defined as the temperature at the maximum slope $|dM/dT|$ derived from the M_{FC} (T) curve at $H = 0.1$ T, as shown in the inset of Fig. 2(a). The higher magnetic transition temperature, T_N ($= 282$ K), corresponds to PM to AFM transition, which is suggested to originate from the AFM exchange interaction through Cr^{3+}–O–Cr^{3+} of Cr_2O_3. The lower magnetic transition, T_C ($= 105$ K), corresponds to AFM to FM transition. It is well known that $LaCrO_3$ has a G-type AFM ground state and Cr_2O_3 is an antiferromagnet with a Néel temperature of 307 K [16,17]. So the appearance of the ferromagnetism in the sample $La_{0.7}Te_{0.3}CrO_3$ is undoubted induced by the Te doping in $LaCrO_3$. For the sake of the charge neutrality, the mixed-valence state of Cr^{2+}–Cr^{3+} is introduced in $La_{0.7}Te_{0.3}CrO_3$ where Te^{4+} ions are used to replace La^{3+} ions. Note that Cr^{3+}/Cr^{2+} ions have the identical electronic configuration with Mn^{4+}/Mn^{3+} ions and the $Cr^{2+}(t_{2g}^3 e_g^1)$ ion is also the Jahn–Teller ion similar to the Mn^{3+} ion, so we consider that the ferromagnetism in $La_{0.7}Te_{0.3}CrO_3$ may originate from the exchange interaction through Cr^{2+}–O–Cr^{3+}.

The magnetization as a function of the applied magnetic field M (H) at 5 K is shown in Fig. 3. It shows that the magnetization does not reach saturation at $H = 4.5$ T, which is considered as a result of the ex-

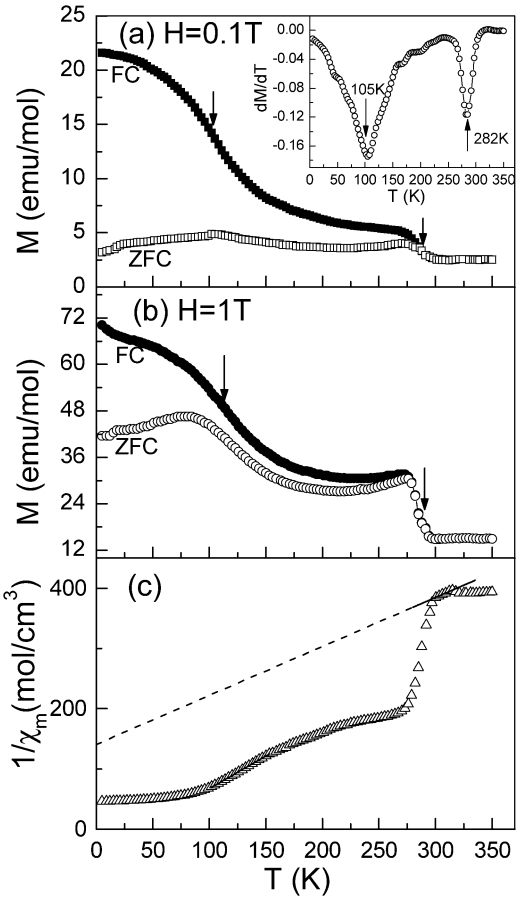

Fig. 2. Magnetization as a function of temperature for $La_{0.7}Te_{0.3}CrO_3$ measured at (a) $H = 0.1$ T and (b) 1 T under the field-cooled (FC) and zero-field-cooled (ZFC) modes that are denoted as the square and circle symbols, respectively. The arrows are denoted as the temperature of magnetic transitions. The inset in (a) shows the temperature dependence of dM/dT for $La_{0.7}Te_{0.3}CrO_3$. (c) The temperature dependence of the inverse of the magnetic susceptibility for $La_{0.7}Te_{0.3}CrO_3$. The solid lines are the calculated curves according to the Curie–Weiss law and the dashed lines represent the extrapolation lines.

istence of the AFM phase in the sample. Moreover, the curve is not linear and the behavior is not reversible implying the existence of a ferromagnetic component in the magnetic moment of chromium. It is calculated to be $0.011\mu_B$/Cr from the extrapolation lines of $M(H)$ curve. All these reveal a superposition of both FM and AFM components. The coexistence of competing FM and AFM exchange interactions would favor the formation of a cluster glass state, as observed in

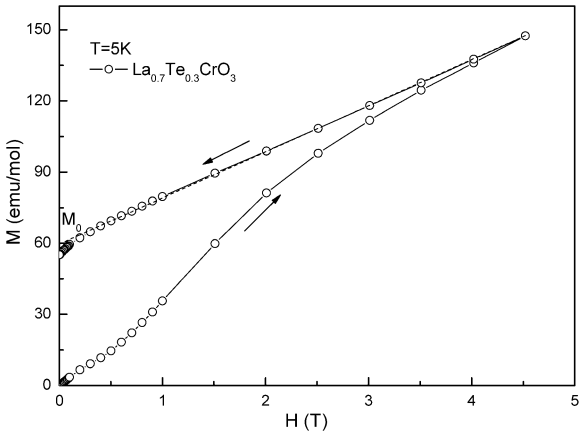

Fig. 3. Field dependence of the magnetization in $La_{0.7}Te_{0.3}CrO_3$ at 5 K. The arrows mark the direction of increasing and decreasing magnetic fields. The dashed lines represent the extrapolation lines and M_0 denotes a linear extrapolation $M(H)$ to $H = 0$.

Fig. 2. In fact, based on the temperature and magnetic field dependence of magnetization for the compound $La_{0.7}Te_{0.3}CrO_3$, the microscopic magnetic structure at low temperatures can be understood by presence of FM clusters in the AFM matrix, which can be clearly observed from the broad magnetic transition range for the sample.

Though we have recognized that the exchange coupling between Cr^{2+}–O–Cr^{3+} can give rise to ferromagnetism, whether its nature stems from double exchange (DE) or superexchange interactions cannot be concluded merely from magnetization measurements. It is well known that a prominent feature of the DE interaction is the intimately correlation between the metallic conduction and the ferromagnetism. So, a detailed study of the transport and magnetoresistance properties is necessary to obtain further insight.

Fig. 4 shows the temperature dependence of resistivity $\rho(T)$ for the sample $La_{0.7}Te_{0.3}CrO_3$ at zero fields. The resistance at low temperatures is so high that the data are collected merely in a limited temperature range in order to avoid exceeding our measuring limit. It shows that $\rho(T)$ curve displays the semiconducting behavior ($d\rho/dT < 0$) over whole measured temperature range. The resistance under an applied field of 4.5 T is almost as same as the resistance under zero fields (not shown here). In other words, no magnetoresistance effect is observed within

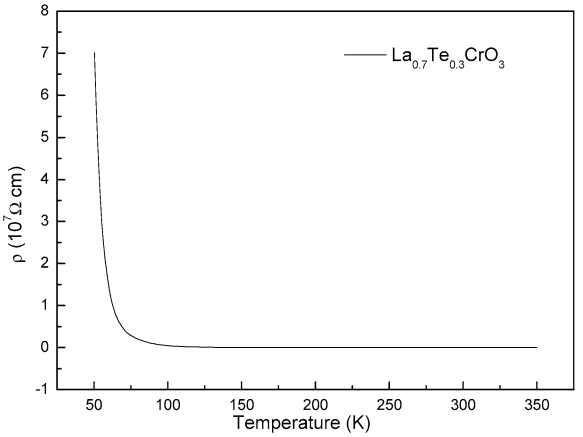

Fig. 4. Temperature dependence of the resistivity of $La_{0.7}Te_{0.3}CrO_3$ at zero applied fields.

measured magnetic field range. This FM insulating (FMI) phase was also found in $La_{1-x}Sr_xMnO_3$ [18], $La_{1-x}Li_xMnO_3$ [19] and $La_{0.9}Te_{0.1}MnO_y$ [20] compounds. FMI behavior cannot be explained based only on the DE model because the FM and metallic nature must coexist within the framework of the DE model. Therefore, the FM order at low temperatures for the sample $La_{0.7}Te_{0.3}CrO_3$ does not mainly originate from DE interaction, but from the quasistatic model for superexchange interaction between Mn^{3+} ions in the case of removing cooperative static Jahn–Teller distortion predicted by Goodenough [21]. Similarly, for the sample $La_{0.7}Te_{0.3}CrO_3$, the observed FM transition may be related to the appearance of SFM arising from the substitution of smaller Te^{4+} ions for larger La^{3+} ions.

In summary, we have studied the structural, magnetic and transport properties of $La_{0.7}Te_{0.3}CrO_3$. The sample has an orthorhombic lattice with the space group *Pbnm*. The sample undergoes two magnetic transitions: the high temperature magnetic transition, corresponds to PM to AFM transition with T_N (= 282 K), and the low temperature magnetic transition corresponds to AFM to FM transition with T_C (= 105 K), which is suggested to be related to the exchange interaction through Cr^{2+}–O–Cr^{3+}. Additionally, $\rho(T)$ curve displays the semiconducting behavior ($d\rho/dT < 0$) over whole measured temperature range, which is suggested to stem from the appearance of SFM insulating phase caused by Te-doping.

Acknowledgements

This work was supported by the National Key Research under contract No. 001CB610604, and the National Nature Science Foundation of China under contract No. 10174085, Anhui Province NSF Grant No. 03046201 and the Fundamental Bureau Chinese Academy of Sciences.

References

[1] S. Geller, Acta Crystallogr. 10 (1957) 243.
[2] W.C. Koehler, E.O. Wollan, J. Phys. Chem. Solids 2 (1957) 100.
[3] K. Ueda, H. Tabata, T. Kawai, Science 280 (1998) 1064.
[4] W. Feduska, A.O. Isenberg, J. Powder Source 10 (1983) 89.
[5] N.Q. Minh, J. Am. Ceram. Soc. 76 (1993) 563.
[6] M. Mori, Y. Hiei, N.M. Sammes, Solid State Ionics 123 (1999) 103.
[7] S. Tanasescu, D. Berger, D. Neiner, N.D. Totir, Solid State Ionics 157 (2003) 365.
[8] P. Duran, J. Tartaj, F. Capel, C. Moure, J. Eur. Ceram. Soc. 24 (2004) 2619.
[9] X. Liu, W. Su, Z. Lu, J. Phys. Chem. Solids 62 (2001) 1919.
[10] X. Liu, W. Su, Z. Lu, J. Alloys Compd. 305 (2000) 21.
[11] L. Groupp, H.U. Anderson, J. Am. Ceram. Soc. 59 (1976) 449.
[12] M. Verelst, N. Rangavittal, C.N. Rao, A. Rousset, J. Solid State Chem. 104 (1993) 74;
I.G. Deac, S.V. Diaz, B.G. Kim, S.-W. Cheong, P. Schiffer, Phys. Rev. B 65 (2002) 174426.
[13] J. Yang, W.H. Song, Y.Q. Ma, R.L. Zhang, Y.P. Sun. J. Magn. Magn. Mater. 285 (2005) 417.
[14] D.B. Wiles, R.A. Young, J. Appl. Crystallogr. 14 (1981) 149.
[15] J.A. Mydosh, in: Spin Glass: An Experimental Introduction, Taylor and Francis, London, 1993.
[16] T.R. McGuire, E.J. Scott, F.H. Graunis, Phys. Rev. 102 (1956) 1000.
[17] P.H. Fang, W.S. Brower, Phys. Rev. 129 (1963) 1963.
[18] J.F. Mitchell, D.N. Argyriou, C.D. Potter, D.G. Hinks, J.D. Jorgensen, S.D. Bader, Phys. Rev. B 54 (1996) 6172.
[19] S.L. Ye, W.H. Song, J.M. Dai, S.G. Wang, K.Y. Wang, C.L. Yuan, Y.P. Sun, J. Appl. Phys. 88 (2000) 5915.
[20] J. Yang, W.H. Song, R.L. Zhang, Y.Q. Ma, B.C. Zhao, Z.G. Sheng, G.H. Zheng, J.M. Dai, Y.P. Sun, Solid State Commun. 31 (2004) 393.
[21] J.B. Goodenough, in: Magnetism and the Chemical Bond, Interscience, New York, 1963.